

## **General Disclaimer**

### **One or more of the Following Statements may affect this Document**

- This document has been reproduced from the best copy furnished by the organizational source. It is being released in the interest of making available as much information as possible.
- This document may contain data, which exceeds the sheet parameters. It was furnished in this condition by the organizational source and is the best copy available.
- This document may contain tone-on-tone or color graphs, charts and/or pictures, which have been reproduced in black and white.
- This document is paginated as submitted by the original source.
- Portions of this document are not fully legible due to the historical nature of some of the material. However, it is the best reproduction available from the original submission.

(NASA-CR-175620) SIMPLE THEORETICAL MODELS  
FOR COMPOSITE ROTOR BLADES Final Report  
(Georgia Inst. of Tech.) 35 p HC A03/MF A01  
CSCL 01C

N85-22382

Unclas  
G3/05 14765

"SIMPLE THEORETICAL MODELS FOR COMPOSITE ROTOR BLADES"

R. Rao Valisetty and Lawrence W. Rehfield  
Center for Rotary Wing Aircraft Technology  
School of Aerospace Engineering  
Georgia Institute of Technology  
Atlanta, Georgia 30332



Final Report  
Grant No. NAG-1-398  
November 1984



## PREFACE

This report summarizes the development of theoretical rotor blade structural models for designs based upon composite construction. Care has been exercised to include a number of nonclassical effects that the author's previous experience indicated would be potentially important to account for. A model, representative of the size of a main rotor blade, is analyzed in order to assess the importance of various influences. The findings of this model study suggest that for the slenderness and closed cell construction considered, the refinements are of little importance and a classical-type theory is adequate. The potential of elastic tailoring is dramatically demonstrated, so the generality of arbitrary ply layup in the cell wall is needed to exploit this opportunity.

## INTRODUCTION

Composite material systems are now the primary materials for helicopter rotor system applications. Bearingless rotor designs proposed for the LHX helicopter are an example. In addition to reduced weight and increased fatigue life, these materials provide designs with fewer parts which means increased service life and improved maintainability. Also, in terms of manufacturing, it is possible to achieve more general aerodynamic shapes including flapwise variation in planform, section and thickness.

The aeroelastic environment in which rotor blades operate consists of inertial, aerodynamic and elastic loadings. Because of the directional nature of the composite materials, it is possible to construct rotor blades with different ply orientations and hybrid combinations of materials exhibiting coupling between various elastic modes of deformation. For example, if the fibers are placed asymmetrically in the upper and lower portions of the blade, there will be a twist induced by flapwise bending. This provides a potential for improving the performance of a lifting surface through aeroelastic tailoring of the primary load-bearing structure. Aeroelastic tailoring of a composite structure involves a design process in which the materials and dimensions are selected to yield specific coupling characteristics which in turn enhance the overall performance of the structure. The design of such advanced structures requires simple and reliable analytical tools which can take into consideration the directional nature of these materials. In this report, a comprehensive bending theory is presented to aid in the design of composite rotor blades.

Most of the existing analyses are formulated for isotropic metal blades. A general tendency is to extend these analyses to composite blades with bending and shear stiffnesses appropriately modified. This, however, does not describe the

anisotropic character of the composites. One of the earlier efforts to account for this particular feature of composite wings is made by Weisshaar<sup>1</sup>. He has developed an engineering theory incorporating the bending-torsion coupling effect for the study of divergence of swept forward wings. Later Mansfield and Sobey<sup>2</sup> have presented an account of the stiffness characteristics of a cylindrical tube representing a helicopter blade composed of a number of plies of arbitrary layout. This theory is derived within the context of Batho-Bredt engineering analysis of thin walled structures and small displacements.

The above theories appear to be adequate for predicting the overall response of slender blades. These theories, however, do not have the capability to predict the stresses or the response with adequate precision when the blade is not slender. A complex three-dimensional stress field develops in such blades which is further complicated by the anisotropy of the materials and inhomogeneity of blade construction. Finite element analyses are reported in Refs. (3) and (4) to obtain stiffnesses and stresses for thick walled blades. For an accurate determination of the stresses, one needs to employ a large number of elements which makes this type of analyses computationally unacceptable for design purposes.

Hong and Chopra<sup>5</sup> have studied the effects of fiber orientation on the flutter of rotor blades. This analysis is based on the nonlinear kinematics of Hodges and Dowell<sup>6</sup>.

Recent theoretical research<sup>7</sup> has contributed a new appreciation for other nonclassical effects in addition to transverse shear deformation in bending-related behavior. A nonclassical contribution to axial stress and transverse normal strain affect response in planar bending situations significantly for certain combinations of geometry and stiffness for homogeneous structures. Incorporating these influences, theories were developed for homogeneous plates<sup>8</sup>, stiffened plates<sup>9</sup> and

laminates<sup>10,11</sup>. Figure 1 depicts the response contributions incorporated in these theories. Stresses and displacements are improved beyond linear (with respect to thickness coordinate) distributions, yet the overall equations retain the character of an engineering theory. This is a distinguishing feature for it allows the integration of nonclassical influences on a simple basis.

The nonclassical influences relevant to rotor blades are those due to transverse shear, bending-related warping, stretching-related warping and torsion related warping. Laminated composites are in general strong and stiff in the plane of lamination and weak and flexible in the transverse direction. Consequently, transverse shear deformation becomes much more pronounced. Bending-related section warping also affects response in a similar way, but it is due to the fact that bending strain does not strictly correspond to planar deformation. Torsion-related warping arises whenever a section is restrained against out of plane deformation. The key to improving the stress predictive capability of a theory is to account for these effects correctly. With this background, the present work is undertaken. A comprehensive theory is developed within the context of small displacements for a single cell composite blade model. The distributions for the warping displacement, axial stress and shear flow are improved.

The starting point is the engineering theory of Mansfield and Sobey<sup>1</sup>. The kinematic procedure to develop the equations follows that of Ref. (8). An example is presented to illustrate the potential for aeroelastic tailoring and the significance of nonclassical influences for rotor blades.

## OVERVIEW

A typical composite rotor blade cross section appears in Figure 2. For a preliminary design, it is common to consider the forward structural box as the primary stiffness producing and load bearing structure. The remaining structure is

considered only as a mass contribution, along with tuning weight which is added to favorably alter the dynamic characteristics. Therefore, the foregoing development is for a single cell beam which is shown in Figure 3 together with a reference coordinate axes system.

The classical development of the theory of thin walled beams under combined loading is based on two hypotheses. The first one is the Euler-Bernoulli hypothesis which states that plane cross sections normal to the axis of the beam remain plane during bending-related deformation and that these sections remain undistorted in their own plane. The second one is due to Saint-Venant which states that the applied torque is carried by a uniform shear flow and the cross sections are free to warp in torsion-related deformation. According to the first hypothesis, the only significant stress is the axial stress,  $\sigma_x$ . This stress is effective in carrying bending and stretching-related loads. For thin walled beams, these assumptions lead to the following results:

$$u(x, y, z) = U - yV_{,x} - zW_{,x} - 2\omega \phi_{,x} \tag{1}$$

$$v(x, y, z) = V - z\phi \tag{1a}$$

$$w(x, y, z) = W - y\phi \tag{1b}$$

$$N_{xs} = \frac{M_x}{2\bar{\Omega}} \tag{2}$$

where  $\omega = \frac{1}{2} \int r ds$  (2a)

Here,  $u$ ,  $v$  and  $w$  denote the components of displacement of any point on the cross section in the directions of the coordinate axes  $x$ ,  $y$  and  $z$ , respectively. Similarly,  $U$ ,  $V$  and  $W$  represent the respective displacement components of the origin of the  $(x, y, z)$  coordinate system. The twist of the cross section is denoted by  $\phi$ . In Saint-Venant-type torsion, the variation of this variable is linear with respect to

the axial coordinate,  $x$ .  $U$ ,  $V$ ,  $W$  and  $\phi$  are functions of  $x$  only. It is convenient to describe the variation of any given parameter on the cross section with respect to a circumferential coordinate,  $s$ , whose origin can be arbitrarily selected. As shown in Figure 3, the perpendicular from the origin of the  $(x, y, z)$  coordinate system on to the tangent at any point  $s$  on the circumference is denoted by  $r$ .  $N_{xs}$  is the shear flow. It is the shear stress resultant per unit length of circumference.  $M_x$  is the applied torque and  $\bar{\Omega}$  is the area enclosed by the box.

There are additional assumptions made regarding the stress state in the structure. Let  $s$  and  $n$  denote circumferential and tangential coordinates so that  $(x, s, n)$  forms an orthogonal coordinate system. With respect to this coordinate system,  $\sigma_x$  and  $\sigma_{xs}$  are the dominant stresses in the structure. The axial stress,  $\sigma_x$ , is due to bending and stretching and the shear stress,  $\sigma_{xs}$ , is due to the applied torque. In the classical development, the remaining stresses --  $\sigma_n$ ,  $\sigma_s$ ,  $\sigma_{ns}$  and  $\sigma_{xn}$  are assumed to be zero because their influence on the response is negligible. This is justified for the following reasons.

In view of the nature of the construction, the structure cannot develop and support  $\sigma_{ns}$ . Therefore, this stress is neglected. The skin of the structure is usually very thin. Therefore, the skin is assumed to be in a state of plane stress with respect to the  $n$ -coordinate direction, which means that  $\sigma_n$  and  $\sigma_{nx}$  are zero. It is essential for the aerodynamic reasons to preserve the airfoil shape. The rigidity of the cross section is maintained by an internal structure, such as a honeycomb filling which does not add measurably to the overall stiffness of the structure. Therefore, the circumferential normal stress,  $\sigma_s$ , cannot develop. It is also not possible to account for this stress within the limitations of a one-dimensional theory. In the new theory, these stress assumptions are retained.

In order to account for the transverse shear, bending-related section warping and torsion-related section warping, a priori knowledge of  $\sigma_x$  and  $\sigma_{xs}$

is necessary. Statically equilibrating stresses can be developed based on the assumptions given by Equations (1) and (2). As a first approximation, it is assumed that these stresses are sufficient to estimate the nonclassical effects. A brief summary of the procedure for developing these stresses follows. This procedure is similar to that of Mansfield and Sobey<sup>1</sup> up to Equation (16). It serves to introduce notation and provides a basis for the new theory. A flow diagram of the subsequent development of the new theory is shown in Figure 4.

### DEVELOPMENT OF ENGINEERING STRESSES

The skin of the single cell tube is considered to be a laminate built from distinctly different layers or lamina. For a typical lamina within this laminate, the relationship between stresses and strains referred to  $x, s$  coordinate system may be expressed in the following matrix form

$$\begin{Bmatrix} \sigma_x \\ \sigma_s \\ \sigma_{xs} \end{Bmatrix} = \begin{bmatrix} Q_{11} & Q_{12} & Q_{16} \\ Q_{12} & Q_{22} & Q_{26} \\ Q_{16} & Q_{26} & Q_{66} \end{bmatrix} \begin{Bmatrix} \epsilon_x \\ \epsilon_s \\ \gamma_{xs} \end{Bmatrix} \quad (3)$$

Where  $\epsilon_x$  and  $\epsilon_s$  are the normal strains in  $x$  and  $s$  coordinate directions.  $\gamma_{xs}$  is the engineering shear strain along the contour of the cross section.  $Q_{ij}$  are the stiffnesses which depend upon the fiber orientation and elastic moduli of the lamina. Equation (3) is derived in Ref. (12).

Now, the layers are assumed to deform together so that the skin can be represented as a homogeneous anisotropic material represented by averaged material properties. Let  $N_s$ ,  $N_x$  and  $N_{xs}$  be the stress resultants per unit length in  $s$ -coordinate direction. Then,

$$\begin{Bmatrix} N_x \\ N_s \\ N_{xs} \end{Bmatrix} = \begin{bmatrix} A_{11} & A_{12} & A_{16} \\ A_{12} & A_{22} & A_{26} \\ A_{16} & A_{26} & A_{66} \end{bmatrix} \begin{Bmatrix} \epsilon_x \\ \epsilon_s \\ \gamma_{xs} \end{Bmatrix} \quad (4)$$

Where

$$A_{ij} = \sum_{k=1}^N \int Q_{ij}^{(k)} dn; \quad i,j=1,2, \text{ and } 6 \quad (5)$$

and  $N$  denotes the number of layers in the skin.  $N_s$  is negligible in unpressurized slender structures, so it is set to zero. Equation (4) is contracted to the following result:

$$\begin{Bmatrix} N_x \\ N_{xs} \end{Bmatrix} = \begin{bmatrix} A_{11} - A_{12}A_{12}/A_{22} & A_{16} - A_{12}A_{26}/A_{22} \\ A_{16} - A_{12}A_{26}/A_{22} & A_{66} - A_{26}A_{26}/A_{22} \end{bmatrix} \begin{Bmatrix} \epsilon_x \\ \gamma_{xs} \end{Bmatrix} \quad (6)$$

It is convenient to have Equation (6) expressed in the following form:

$$\begin{Bmatrix} N_x \\ \gamma_{xs} \end{Bmatrix} = \begin{bmatrix} H_{11} & H_{21} \\ H_{21} & H_{22} \end{bmatrix} \begin{Bmatrix} \epsilon_x \\ N_{xs} \end{Bmatrix} \quad (7)$$

where

$$\begin{aligned} H_{22} &= 1/(A_{66} - A_{26}A_{26}/A_{22}) \\ H_{21} &= -(A_{16} - A_{12}A_{26}/A_{22})H_{22} \\ H_{11} &= A_{11} - A_{12}A_{12}/A_{22} + (A_{16} - A_{12}A_{26}/A_{22})H_{21} \end{aligned} \quad (8a)$$

The resultant loads acting on a given cross section are defined by the following integrals:

$$(N, M_y, M_z) = \oint N_x(u, z, y) ds \quad (8b)$$

Where,  $N$  is the tensile load along  $x$ -axis,  $M_y$  is the bending moment about  $y$ -axis and  $M_z$  is the bending moment about  $z$ -axis.

The location of the origin of the  $y, z$  axes and their orientation are at present arbitrary. The ensuing analysis is greatly simplified if they are selected so that

$$\oint (y, z, yz) H_{11} ds = (0, 0, 0) \quad (9)$$

The resulting locus of origins of each section, then, defines the tension axis of the blade and the new  $y, z$  axes are the principal axes of bending. Now the stress resultants are evaluated with the aid of equations (1) and (7).

$$N = U_{,x} \oint H_{11} ds - \frac{M_x}{2\bar{\Omega}} \oint H_{21} ds \quad (10)$$

$$M_y = -W_{,xx} \oint H_{11} z^2 ds - \frac{M_x}{2\bar{\Omega}} \oint H_{21} z ds \quad (11)$$

$$M_z = -V_{,xx} \oint H_{11} y^2 ds - \frac{M_x}{2\bar{\Omega}} \oint H_{21} y ds \quad (12)$$

Since the cross sections undergo only a rigid body rotation and also because the axial displacement,  $u$ , is continuous along the contour of the cross section, the rate of twist is evaluated from the following formula<sup>(13)</sup>

$$\phi_{,x} = \frac{1}{2\bar{\Omega}} \oint \gamma_{xs} ds \quad (13)$$

and Equations (1) and (7) to obtain

$$\begin{aligned} \phi_{,x} = & (U_{,x} \oint H_{21} ds - W_{,xx} \oint H_{21} z ds \\ & - V_{,xx} \oint H_{21} y ds + \frac{M_x}{2\bar{\Omega}} \oint H_{22} ds) / 2\bar{\Omega} \end{aligned} \quad (14)$$

Equations (2), (10), (11), (12) and (14) are now recast in the following form to obtain

the overall engineering elastic law for the structure

$$\begin{Bmatrix} U_{,x} \\ -W_{,xx} \\ -V_{,xx} \\ \phi_{,x} \end{Bmatrix} = \begin{bmatrix} S_{11} & 0 & 0 & S_{14} \\ 0 & S_{22} & 0 & S_{24} \\ 0 & 0 & S_{33} & S_{34} \\ S_{14} & S_{24} & S_{34} & S_{44} \end{bmatrix} \begin{Bmatrix} N \\ M_y \\ M_z \\ M_x \end{Bmatrix} \quad (15)$$

$S$  is a symmetric flexibility matrix whose nonzero elements are given by

$$S_{11} = 1/\oint H_{11} ds$$

$$S_{14} = S_{11}/(2\bar{\Omega} \oint H_{21} ds)$$

$$S_{22} = 1/\oint H_{11} z^2 ds$$

$$S_{24} = S_{22}/(2\bar{\Omega} \oint H_{21} z ds)$$

$$S_{33} = 1/\oint H_{11} y^2 ds$$

$$S_{34} = S_{33}/(2\bar{\Omega} \oint H_{22} y ds)$$

$$S_{44} = \frac{1}{4\bar{\Omega}^2} \oint H_{22} ds + \frac{1}{2\bar{\Omega}} S_{14} \oint H_{21} ds$$

$$+ \frac{1}{2\bar{\Omega}} S_{24} \oint H_{21} z ds + \frac{1}{2\bar{\Omega}} S_{24} \oint H_{21} y ds \quad (16)$$

The development described so far is reported in Ref. (1). The constitutive equations (15) are to be supplemented with the following equilibrium equations

$$N_{,x} + n_x = 0 \quad (17)$$

$$M_{y,x} = Q_z \quad (18)$$

$$M_{z,x} = Q_y \quad (19)$$

$$Q_{z,x} + q_z = 0 \quad (20)$$

$$Q_{y,x} + q_y = 0 \quad (21)$$

$$M_{x,x} + m_x = 0 \quad (22)$$

to form the engineering theory for single cell laminated beams under combined loading. Here,  $n_x$  represents the intensity of axial distributed loading,  $Q_z$  and  $Q_y$  represent shear stress resultants,  $q_z$  and  $q_y$  represent the distributed loads and  $m_x$  represents the distributed torque.

In order to proceed with the development of the new theory, it is necessary to have statically equilibrating stress resultants. The axial stress resultant can be represented in terms of overall stress resultants with the aid of Equations (15), (1) and (7)

$$N_x = f_1 N + f_2 M_y + f_3 M_z + f_4 M_x \quad (23)$$

where

$$\begin{aligned} f_1 &= H_{11} S_{11} \\ f_2 &= z H_{11} S_{22} \\ f_3 &= y H_{11} S_{33} \\ f_4 &= H_{11} S_{14} + z H_{11} S_{24} + y H_{11} S_{34} - H_{21} / 2 \bar{\Omega} \end{aligned} \quad (24)$$

The nonuniform shear flow due to bending and stretching can be derived from the following equilibrium equation

$$N_{x,x} + N_{xs,s} = 0 \quad (25)$$

and an additional requirement that the shear flow be equivalent to the applied torque. This result can be given as

$$N_{xs} = \frac{M_x}{2\bar{\Omega}} - \int N_{x,x} ds + \frac{1}{2\bar{\Omega}} \oint r ds \int N_{x,x} ds \quad (26)$$

With  $r$  denoting the perpendicular from the origin to the tangent at  $s$ . The axial stress term can be eliminated from above with the aid of Equation (25).

$$N_{xs} = \frac{M_x}{2\bar{\Omega}} - f_5 N_{,x} - f_6 M_{y,x} - f_7 M_{z,x} - f_8 M_{x,x} \quad (27)$$

where

$$f_i = \int f_{(i-4)} ds - \frac{1}{2\bar{\Omega}} \oint r ds \int f_{(i-4)} ds \quad ; i=5,6,7,8 \quad (28)$$

Equations (23) and (27) provide stress resultants which are in static equilibrium. A comparison of Equations (2) and (27) reveals that the two expressions for the shear flow are different. The new shear flow is nonuniform along the contour of the cross section and this is due to bending and stretching loads. The nonuniform shear flow in turn affects the twist; its contribution can be evaluated from Equations (13), (7), (15) and (28). The result can be expressed as

$$\begin{aligned} \phi_{,x} = & S_{14}N + S_{24}M_y + S_{34}M_z + S_{44}M_x \\ & + f_9 N_{,x} + f_{10} M_{y,x} + f_{11} M_{z,x} + f_{12} M_{x,x} \end{aligned} \quad (29)$$

where

$$f_i = -\frac{1}{2\bar{\Omega}} \oint H_{21} f_{(i-4)} ds \quad ; i=9,10,11,12 \quad (30)$$

$f_{10}$  and  $f_{11}$  will be zero if the shear resultants pass through the shear center. This does not, however, indicate that twist will not develop under bending and stretching related loads. The presence of coupling includes this possibility.

### DEVELOPMENT OF THE NEW THEORY

The theoretical developmental process is described in the form of a flow chart in Figure 4. The fundamental assumption that permits this development is that the transverse shear strain can be estimated from the statically equivalent stresses given by Equations (23) and (27). It is also assumed that the cross sections undergo a rigid body rotation. If  $\eta$  is the tangential displacement in the  $s$ -direction, then

$$\eta = r\phi \quad (31)$$

The linear strain-displacement relation for the transverse shear strain is given by

$$\gamma_{xs} = u_{,s} + \eta_{,x} \quad (32)$$

The following result emerges upon integration of  $u_{,s}$  with the aid of Equation (31)

$$u = U - zW_{,x} - yV_{,x} - 2\omega\phi_{,x} + \int \gamma_{xs} ds \quad (33)$$

where

$$\omega = \frac{1}{2} \int r ds \quad (34)$$

The first three terms in Equation (33) satisfy the engineering hypothesis that plane cross sections remain plane during deformation. The fourth term denotes the effect of restrained warping and the fifth term contains the effect of transverse shear deformation. With the aid of Equations (7), (10), (15), (27) and (29) the non-classical part of the displacement is expressed in terms of force resultants to arrive at

$$\begin{aligned} u = & U - zW_{,x} - yV_{,x} + f_{13}N + f_{14}M_y + f_{15}M_z + f_{16}M_x \\ & + f_{17}N_{,x} + f_{18}M_{y,x} + f_{19}M_{z,x} + f_{20}M_{x,x} \end{aligned} \quad (35)$$

where

$$\begin{aligned}
f_{13} &= -2\omega S_{14} + \int H_{21} S_{11} ds \\
f_{14} &= -2\omega S_{24} + \int H_{21} S_{22} z ds \\
f_{15} &= -2\omega S_{34} + \int H_{21} S_{22} y ds \\
f_{16} &= -2\omega S_{44} + \int (H_{21} S_{14} + H_{21} z S_{24} + H_{31} y S_{34} + H_{22}/2\bar{\Omega}) ds \\
f_{17} &= -2\omega f_9 - \int H_{22} f_5 ds \\
f_{18} &= -2\omega f_{10} - \int H_{22} f_6 ds \\
f_{19} &= -2\omega f_{11} - \int H_{22} f_7 ds \\
f_{20} &= -2\omega f_{12} - \int H_{22} f_8 ds
\end{aligned} \tag{36}$$

The new displacement is now used in conjunction with Equations (7) and (26) to compute the axial stress resultant

$$\begin{aligned}
N_x &= H_{11}(U_{,x} - zW_{,xx} - yV_{,xx} + f_{13}N_{,x} + f_{14}M_{y,x} + f_{15}M_{z,x} + f_{16}M_{x,x} \\
&\quad + f_{17}N_{,xx} + f_{18}M_{y,xx} + f_{19}M_{z,xx} + f_{20}M_{x,xx}) \\
&\quad - H_{21}\left(\frac{M_x}{2\bar{\Omega}} - f_5N_{,x} - f_6M_{y,x} - f_7M_{z,x} - f_8M_{x,x}\right)
\end{aligned} \tag{37}$$

The engineering kinematic variables  $U$ ,  $W$ ,  $V$  must be related to the generalized force variables. This is accomplished by enforcing the definitions in Equation (8)

$$\begin{aligned}
(N, M_y, M_z) &= U_{,x} \int H_{11}(l, z, y) ds \\
&\quad - W_{,xx} \int H_{11}(l, z, y) z ds \\
&\quad - V_{,xx} \int H_{11}(l, z, y) y ds \\
&\quad + N_{,x} \int (H_{11} f_{13} + H_{21} f_5)(l, z, y) ds
\end{aligned}$$

$$\begin{aligned}
& + M_{y,x} \int (H_{11} f_{14} + H_{21} f_{16})(l, z, y) ds \\
& + M_{z,x} \int (H_{11} f_{15} + H_{21} f_{17})(l, z, y) ds \\
& + M_{x,y} \int (H_{11} f_{16} + H_{21} f_{18})(l, z, y) ds \\
& + N_{,xx} \int H_{11} f_{17}(l, y, z) ds \\
& + M_{y,xx} \int H_{11} f_{18}(l, y, z) ds \\
& + M_{z,xx} \int H_{11} f_{19}(l, y, z) ds \\
& + M_{x,xx} \int H_{11} f_{20}(l, y, z) ds \\
& + M_x \int (-H_{21}/2 \bar{\Omega})(l, y, z) ds
\end{aligned}$$

(38)

These equations can be cast in a more familiar form by solving them for the engineering kinematic variables.

$$\begin{aligned}
\begin{Bmatrix} U_{,x} \\ -W_{,xx} \\ -V_{,xx} \end{Bmatrix} &= \begin{bmatrix} S_{11} & 0 & 0 & S_{14} \\ 0 & S_{22} & 0 & S_{24} \\ 0 & 0 & S_{33} & S_{34} \end{bmatrix} \begin{Bmatrix} N \\ M_y \\ M_z \\ M_x \end{Bmatrix} \\
&+ \begin{bmatrix} S'_{11} & S'_{12} & S'_{13} & S'_{14} \\ S'_{12} & S'_{22} & S'_{23} & S'_{24} \\ S'_{13} & S'_{23} & S'_{33} & S'_{34} \\ S'_{14} & S'_{24} & S'_{34} & S'_{44} \end{bmatrix} \begin{Bmatrix} N_{,x} \\ M_{y,x} \\ M_{z,x} \\ M_{x,x} \end{Bmatrix}
\end{aligned}$$

$$+ \begin{bmatrix} S''_{11} & S''_{12} & S''_{13} & S''_{14} \\ S''_{12} & S''_{22} & S''_{23} & S''_{24} \\ S''_{13} & S''_{23} & S''_{33} & S''_{34} \\ S''_{14} & S''_{24} & S''_{34} & S''_{44} \end{bmatrix} \begin{Bmatrix} N_{,xy} \\ M_{y,xx} \\ M_{z,xx} \\ M_{x,xx} \end{Bmatrix} \quad (39)$$

Equations (39) describe the stretching and bending of the beam. They replace the classical Equations (15). The additional flexibility matrices  $[S']$  and  $[S'']$  depend only on the elastic moduli of the material and dimensions of the cross section. The expressions for these parameters can easily be deduced. For example

$$S'_{11} = (1/\oint H_{11} ds) / \oint (H_{11} f_{13} + H_{21} f_5) ds, \quad \text{etc.} \quad (40)$$

The axial stress resultant may be expressed in terms of generalized force variables with the aid of Equations (39) and (37)

$$\begin{aligned} N_x = & f_1 N + f_2 M_y + f_3 M_z + f_4 M_x \\ & + f_{21} N_{,x} + f_{22} M_{y,x} + f_{23} M_{z,x} + f_{24} M_{x,x} \\ & + f_{25} N_{,xx} + f_{26} M_{y,xx} + f_{27} M_{z,xx} + f_{28} M_{x,xx} \end{aligned} \quad (41)$$

where

$$\begin{aligned} f_{21} &= H_{11}(S'_{11} + zS'_{12} + yS'_{13} + f_{13}') + H_{21}f_5 \\ f_{22} &= H_{11}(S'_{12} + zS'_{22} + yS'_{23} + f_{14}') + H_{21}f_6 \\ f_{23} &= H_{11}(S'_{13} + zS'_{23} + yS'_{33} + f_{15}') + H_{21}f_7 \\ f_{24} &= H_{11}(S'_{14} + zS'_{24} + yS'_{34} + f_{16}') + H_{21}f_8 \\ f_{25} &= H_{11}(S''_{11} + zS''_{12} + yS''_{13} + f_{17}') \end{aligned}$$

$$\begin{aligned}
f_{26} &= H_{11}(S''_{12} + zS''_{22} + yS''_{23} + f_{18}) \\
f_{27} &= H_{11}(S''_{13} + zS''_{23} + yS''_{33} + f_{19}) \\
f_{28} &= H_{11}(S''_{14} + zS''_{24} + yS''_{34} + f_{20})
\end{aligned} \tag{42}$$

The corrections to the axial stress resultant include the effects of bending related warping and torsion-related restrained warping. The new shear flow can now be estimated substituting this stress in Equation (26).

$$\begin{aligned}
N_{xs} &= \frac{M_x}{2\bar{\Omega}} - f_5 N_{,x} - f_6 M_{y,x} - f_7 M_{z,x} - f_8 M_{x,x} \\
&\quad - f_{29} N_{,xx} - f_{30} M_{y,xx} - f_{31} M_{z,xx} - f_{32} M_{x,xx} \\
&\quad - f_{33} N_{,xxx} - f_{34} M_{y,xxx} - f_{35} M_{z,xxx} - f_{36} M_{x,xxx}
\end{aligned} \tag{43}$$

where

$$f_i = \int f_{(i-8)} ds - \frac{1}{2\bar{\Omega}} \oint r ds \int f_{(i-8)} ds \quad i=29, 30, \dots, 36 \tag{44}$$

The rate of twist is re-evaluated with the aid of Equations (13), (7), (35) and (41)

$$\begin{aligned}
\phi_{,x} &= S_{14}N + S_{24}M_y + S_{34}M_z + S_{44}M_x \\
&\quad + f_9 N_{,x} + f_{10} M_{y,x} + f_{11} M_{z,x} + f_{12} M_{x,x} \\
&\quad + f_{37} N_{,xx} + f_{38} M_{y,xx} + f_{39} M_{z,xx} + f_{40} M_{x,xx} \\
&\quad + f_{41} N_{,xxx} + f_{42} M_{y,xxx} + f_{43} M_{z,xxx} + f_{44} M_{x,xxx}
\end{aligned} \tag{45}$$

where

$$\begin{aligned}
f_{37} &= \frac{1}{2\bar{\Omega}} \oint ds \left\{ H_{21}(S''_{11} + zS''_{12} + yS''_{13} + f_{17}) - H_{21}f_{29} \right\} \\
f_{38} &= \frac{1}{2\bar{\Omega}} \oint ds \left\{ H_{21}(S''_{12} + zS''_{22} + yS''_{23} + f_{18}) - H_{21}f_{30} \right\} \\
f_{39} &= \frac{1}{2\bar{\Omega}} \oint ds \left\{ H_{21}(S''_{13} + zS''_{23} + yS''_{33} + f_{19}) - H_{21}f_{31} \right\} \\
f_{40} &= \frac{1}{2\bar{\Omega}} \oint ds \left\{ H_{21}(S''_{14} + zS''_{24} + yS''_{34} + f_{20}) - H_{21}f_{32} \right\} \\
f_i &= \frac{1}{2\bar{\Omega}} \oint ds \left\{ -H_{21}f_{(i-8)} \right\} \quad ; i = 41, 42, 43, 44
\end{aligned} \tag{46}$$

The governing equations for the response of single cell laminated rotor blades can now be summarized. Overall equations of equilibrium remain same as those in (17) - (22). Similarly, the generalized kinematic variables and force variables also remain the same. The kinematic variables are  $U_{,x}$ ,  $-W_{,xx}$ ,  $-V_{,xx}$  and  $\phi_{,x}$ . The force variables are  $N$ ,  $M_y$ ,  $M_z$  and  $M_x$ . Equations that relate these two sets of variables are given by (39) and (45). These overall constitutive equations contain the effects due to transverse shear, torsional shear and restrained warping. New distributions for the axial displacement, axial stress and shear flow are contained in Equations (35), (41) and (44).

#### APPLICATION

The following section provides an example which illustrates the relative significance of nonclassical influences on overall response predictions and stress estimates. The potential for aeroelastic tailoring is also investigated to a limited extent. For this purpose, the rotor blade of Boeing's CH-47 helicopter is used as a

guide in sizing. The blade is modeled as a single cell beam with a uniformly distributed load,  $q_z$ , with  $q$  applied at the quarter-chord point. The end where the blade is joined to the hub is treated as a clamped end, with the other end being free. The dimensions of the box are shown in Figure 5.

In order to study the influence of material properties, two different material systems, graphite/epoxy and glass/epoxy, are selected. The following material properties are assumed for each ply:

Graphite/Epoxy:

$$\begin{aligned} E_1 &= 25 \times 10^6 \text{ psi}, & E_2 &= E_3 = 1 \times 10^6 \text{ psi} \\ G_{23} &= 0.2 \times 10^6 \text{ psi}, & G_{12} &= G_{13} = 0.5 \times 10^6 \text{ psi} \\ \nu_{12} &= \nu_{13} = 0.25, & \nu_{23} &= 0.25 \end{aligned}$$

Glass/Epoxy:

$$\begin{aligned} E_1 &= 7.3 \times 10^6 \text{ psi}, & E_2 &= E_3 = 2.1 \times 10^6 \text{ psi} \\ G_{12} &= G_{13} = 0.88 \times 10^6 \text{ psi} \\ \nu_{12} &= \nu_{13} = 0.275, & \nu_{23} &= 0.25 \end{aligned}$$

The E's are Young's moduli, the G's are shear moduli and  $\nu$ 's are Poisson ratios. The subscript "1" denotes a direction along the fibers, "2" and "3" denote directions normal to the fiber. All plies are identical with a thickness of 0.0085 inches.

Two different layups are considered for the box skin. These are  $(0_{12}, 45_{12})$  and  $(0_{16}, 45_8)$ . The first one is more effective in torsion and the second one in bending. Furthermore, these plies are arranged with respect to  $z = 0$  plane in such a way that there exists three distinctly different couplings between elastic modes of deformation. Because of the nature of the applied loading and skin layup, there is no coupling between stretching and twisting or between bending about z-axis and

twisting. The only coupling is between bending about the y-axis and torsion (flapwise bending). This coupling is controlled by  $S_{24}$ . As shown in Figure 6, three different layups are possible depending upon whether  $45^\circ$  plies are placed symmetrically or antisymmetrically with respect to  $z = 0$  plane.

The first configuration is a balanced design. Since the  $45^\circ$  plies are placed symmetrically,  $S_{24}$  is zero, which means that there is no coupling between bending about y-axis and torsion. The other two designs are unbalanced. Depending on the angle of orientation with respect to the load, these designs produce either enhanced (positive) coupling or reduced (negative) coupling. As shown in the Tables 1-3, there are now twelve different designs depending upon the material system, relative ratio of  $0^\circ$  and  $45^\circ$  plies and relative orientation of the  $45^\circ$  plies in upper and lower parts of the box and placement of the load.

Under the applied uniformly distributed line load ( $q_z = q$ ), all these structures undergo twisting as well as bending about y-axis. Since this is a statically determinate problem, the flapwise bending moment and torque are estimated as

$$M_y = -\frac{q}{2}(x - L)^2$$

$$M_x = -q e(x - L) \quad (47)$$

$e$  is eccentricity of applied loading which in this case is 5 inches, The applicable boundary conditions are given by the following:

$$\text{At } x = 0: W = 0, W_{,x} = 0, \phi = 0 \quad (48)$$

Under these conditions, equilibrium equations (18), (20), (22), the overall

constitutive equations for  $-W_{,xx}$  from (39) and the Equation (45) for twist are solved.

The results for the transverse displacement and the twist at the free end are presented in Tables 1 and 2, respectively. These parameters are given in terms of unit applied load,  $q$ . Similarly, the maximum values for the stress resultants  $N_x$  and  $N_{xy}$  at the root are also presented per unit applied load in Figure 3. The maximum value of the axial stress occurs at the center of the web-like vertical portion of the structure.

The present theory results for  $W$  and  $\phi$  are subdivided into three groups as shown in Tables 1 and 2 to illustrate the improvements due to nonclassical effects and coupling. In the simplest engineering approach, the coupling effects are usually neglected. The material is assumed to be orthotropic, effectively represented by equivalent bending and torsional rigidities. These results are denoted "classical" in Tables 1 and 2. It can be concluded from this study that the nonclassical effects influence deflection more than the coupling parameter and the improvements from both coupling and nonclassical effects are relatively small compared to the classical result. On the other hand, the coupling accounts for a major portion of the twist. If it is not incorporated, major discrepancies arise in the twist predictions. This is because the classical approach cannot delineate between the balanced and unbalanced designs. The nonclassical influences on twist predictions are negligible. With respect to the transverse displacement prediction, it may be seen that the nonclassical influences are more pronounced for graphite/epoxy material system and  $(0_{16}, 45_8)$  layup.

Table 3 shows predictions for the maximum values of the stress resultants. Present theory results are evaluated from Equations (41) and (43). For the sake of comparison, stresses from Mansfield's theory<sup>2</sup> are also presented. These are not available in Ref. (2), but are evaluated using Equations (1), (7) and (15). Unlike the

"classical" results for twist and deflection, Mansfield stresses include the bending-torsion coupling effect. Therefore, the apparent differences between the present theory predictions and those from the Mansfield theory are entirely due to nonclassical influences. Failure to account for these effects leads to an under estimation of the stresses. This could be as much as 4% for tensile stresses and 9% for the compressive stresses.

The structure considered here is very slender. The theory is also developed under the premises of a thin walled cylinder. This explains why the nonclassical influences are so small in this example. Experience<sup>7-10</sup> shows, for beams and plates made of composite materials, the nonclassical influences become important enough to be included as the structure becomes "thicker" on a relative basis. Since the kinematic procedure used here is the same as the one used in Ref. (7)-(10), the present theory can be expected to yield valid results even for very thick-walled rotor blades.

#### SUMMARY AND CONCLUSIONS

A theory has been developed for composite rotor blades that can be modeled as closed cell beams. The theory accounts for nonclassical influences related to restrained warping, transverse shear stain and bending and stretching-related warping. A primary influence that is included is elastic coupling that results from arbitrary composite ply layup in the walls of the cell. To illustrate the role of elastic coupling and nonclassical influences, a rotor blade-type model has been created. This model is analyzed as a single cell cantilever beam under uniformly distributed load. The following conclusions are drawn from this example:

1. Nonclassical influences and elastic coupling have a negligible effect on transverse deflection.
2. Twist is controlled by the elastic coupling. Nonclassical influences have a negligible impact on twist.

3. The axial stress predictions are improved as a result of accounting for the nonclassical influences. The shear flow is affected only slightly by these nonclassical influences.
4. The potential for aeroelastic tailoring has been illustrated by choosing three designs with different layups. The first one is a balanced design with zero coupling. The second and third are unbalanced designs; one of these two produces enhanced coupling and the other reduced coupling. For all of these three designs, the weight is the same and transverse deflection and maximum stresses generated within are also approximately the same, yet the induced twists are different.
5. The structure considered in this example is very slender. This is the reason why the nonclassical influences appear so small in this example. By the experience garnered by the authors with laminated thick plates and beams, it is believed that these influences become more pronounced for thick walled rotor blades and the present theory is capable of predicting them.

### RECOMMENDATIONS

It appears that the nonclassical influences are of little importance in the model. As the model approximates practical dimensions of main rotor blades, it is likely that the slenderness, together with closed cell construction, are responsible for this. As a practical matter, the classical theory of Mansfield and Sobey<sup>2</sup> should be adequate in most cases and should be used.

If the blade under consideration is less "slender" than the example or if moisture-temperature effects significantly alter the stiffness properties of the composite material, then the new theory developed herein can be used. Another situation, the determination of higher than first few vibration modes, also requires the use of the present, more complicated theory.

## REFERENCES

1. Weisshaar, T.A., "Divergence of Forward Swept Composite Wings," Journal of Aircraft, Vol. 17, No. 6, 1980, pp. 442-448.
2. Mansfield, E.H. and Sobey, A.J., "The Fibre Composite Helicopter Blade, Part 1: Stiffness Properties, Part 2: Prospect for Aeroelastic Tailoring," Aeronautical Quarterly, May 1979, pp. 413-449.
3. Wörndle, R., "Calculation of the Cross Section Properties and the Shear Stresses of Composite Rotor Blades," Vertica, Vol. 6, 1982, pp. 111-129.
4. Gia Votto, V., et. al., "Anisotropic Beam Theory and Applications," Computers and Structures, Vol. 16, No. 1-4, pp. 403-413, 1983.
5. Hong, C-H. and Chopra, I., "Aeroelastic Stability Analysis of a Composite Blade," presented at the 40th Annual National Forum of the American Helicopter Society, Crystal City, Virginia, May 16-18, 1984.
6. Hodges, D.H. and Dowell, E.H. "Nonlinear Equations of Motion for the Elastic Bending and Torsion of Twisted Nonuniform Blades," NASA TN D-7818, December 1974.
7. Rehfield, L.W. and Murthy, P.L.N., "Toward a New Engineering Theory of Bending: Fundamentals," AIAA Journal, Vol. 20, No. 5, 1982, pp. 693-699.
8. Rehfield, L.W. and Valisetty, R.R., "A Simple Refined Theory for Bending and Stretching of Homogeneous Plates," AIAA Journal, Vol. 22, No. 1, 1984, pp. 90-95.
9. Yehezkely, O. and Rehfield, L.W., "A New Comprehensive Theory for Bending and Buckling of Stiffened Plates," to appear in Israel Journal of Technology.
10. Rehfield, L.W. and Valisetty, R.R., "A Comprehensive Theory for Planar Bending of Laminates," Computers and Structures, Vol. 16, Nos. 1-4, 1983, pp. 441-447.
11. Valisetty, R.R. and Rehfield, L.W., "A Theory for Stress Analysis of Composite Laminates," presented at the 24th AIAA/ASME/ASCE/AHS Structures, Structural Dynamics and Materials Conference, Lake Tahoe, Nevada, May 2-4, 1983.
12. Jones, R.M., Mechanics of Composite Materials, Scripta Book Company, Washington, D.C., 1975.
13. Oden, J.T., Mechanics of Elastic Structures, McGraw-Hill Book Company, 1967, New York.

List of Figures

- Figure 1. Mechanical Responses Incorporated in the New Theories of Refs. (7)-(11)
- Figure 2. Typical Rotor Blade Cross Section
- Figure 3. Coordinate Systems
- Figure 4. Theory Developmental Process
- Figure 5. CH-47 Rotor Blade Idealized as a Single Cell Form
- Figure 6. Skin Layups

ORIGINAL PAGE IS  
OF POOR QUALITY

FIGURE 1. MECHANICAL RESPONSES INCORPORATED IN THE NEW THEORIES  
OF REFS. (7)-(11)



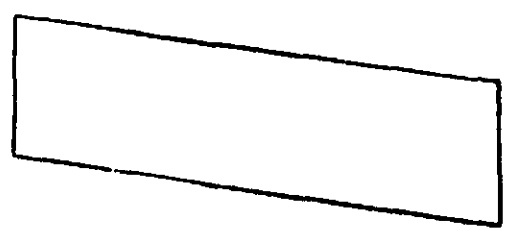
PURE BENDING



PURE STRETCHING



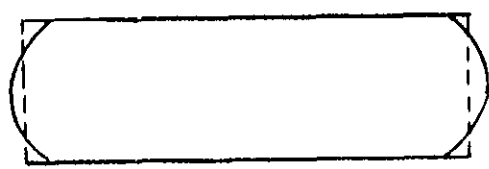
THICKNESS SHEAR



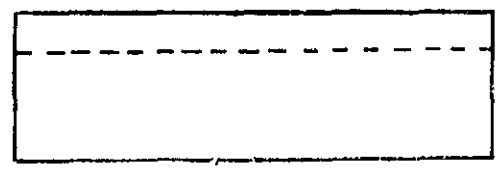
TRANSVERSE SHEAR



BENDING RELATED  
SECTION WARPING



STRETCHING RELATED  
SECTION WARPING



TRANSVERSE  
NORMAL STRAIN

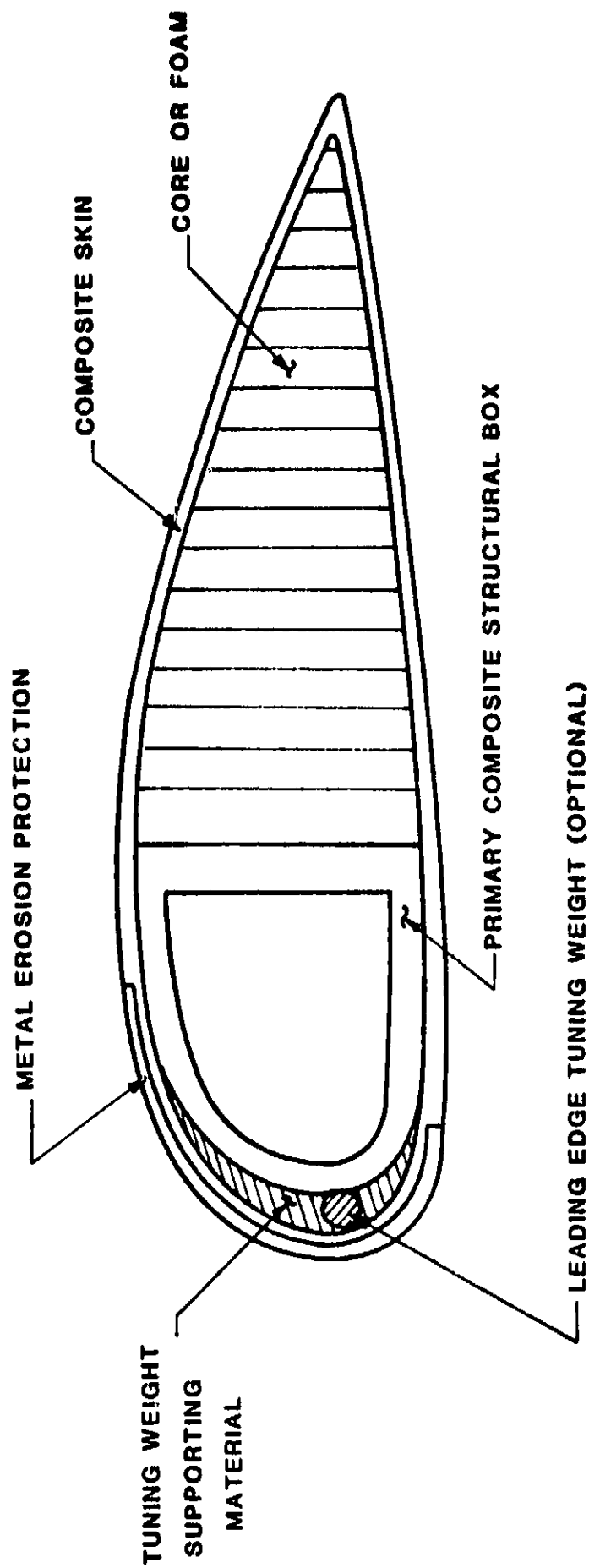


FIGURE 2

# TYPICAL ROTOR BLADE CROSS SECTION

ORIGINAL PAGE IS  
OF POOR QUALITY

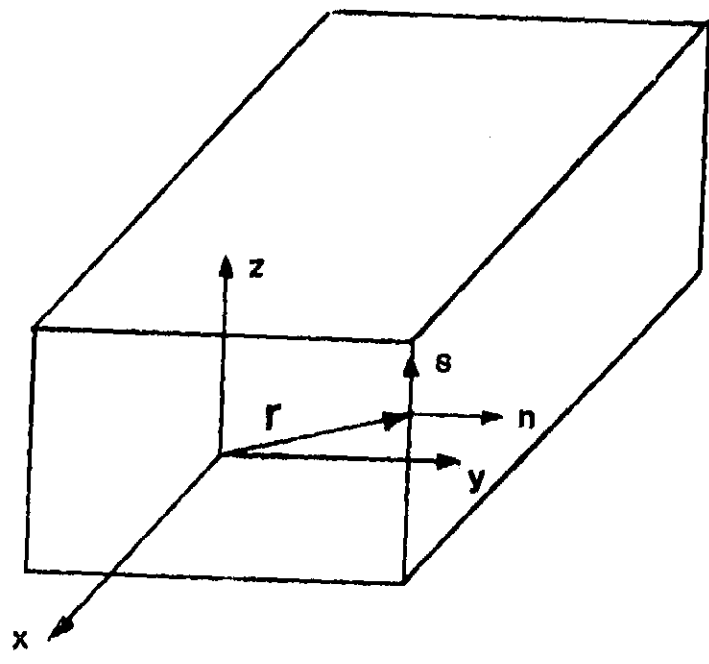
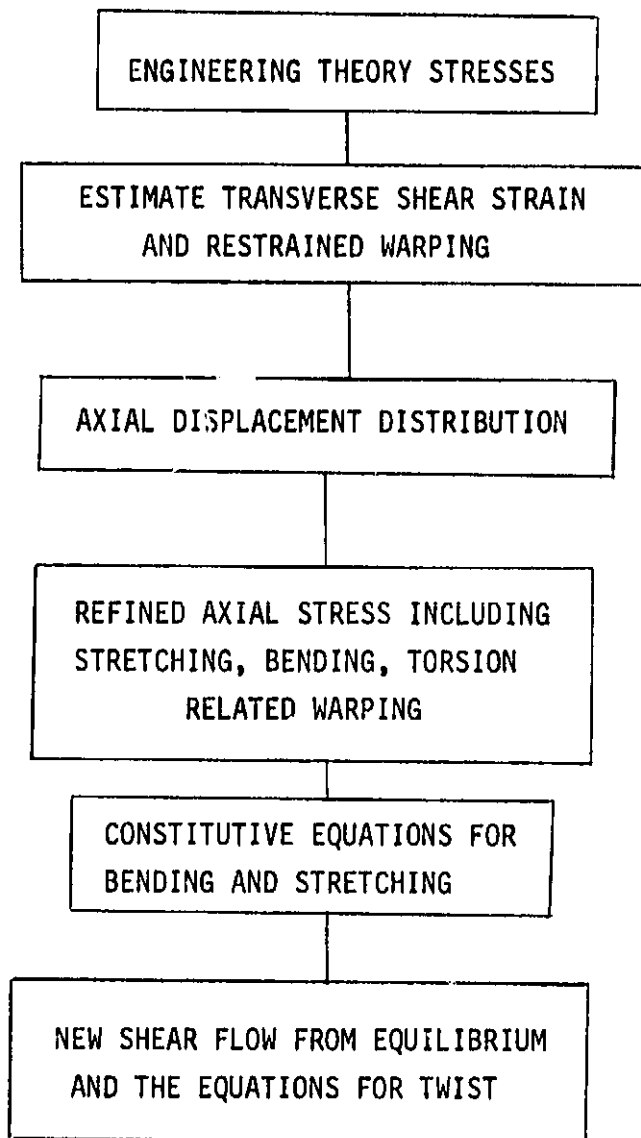


FIGURE 3. COORDINATE SYSTEMS

FIGURE 4. THEORY DEVELOPMENTAL PROCESS



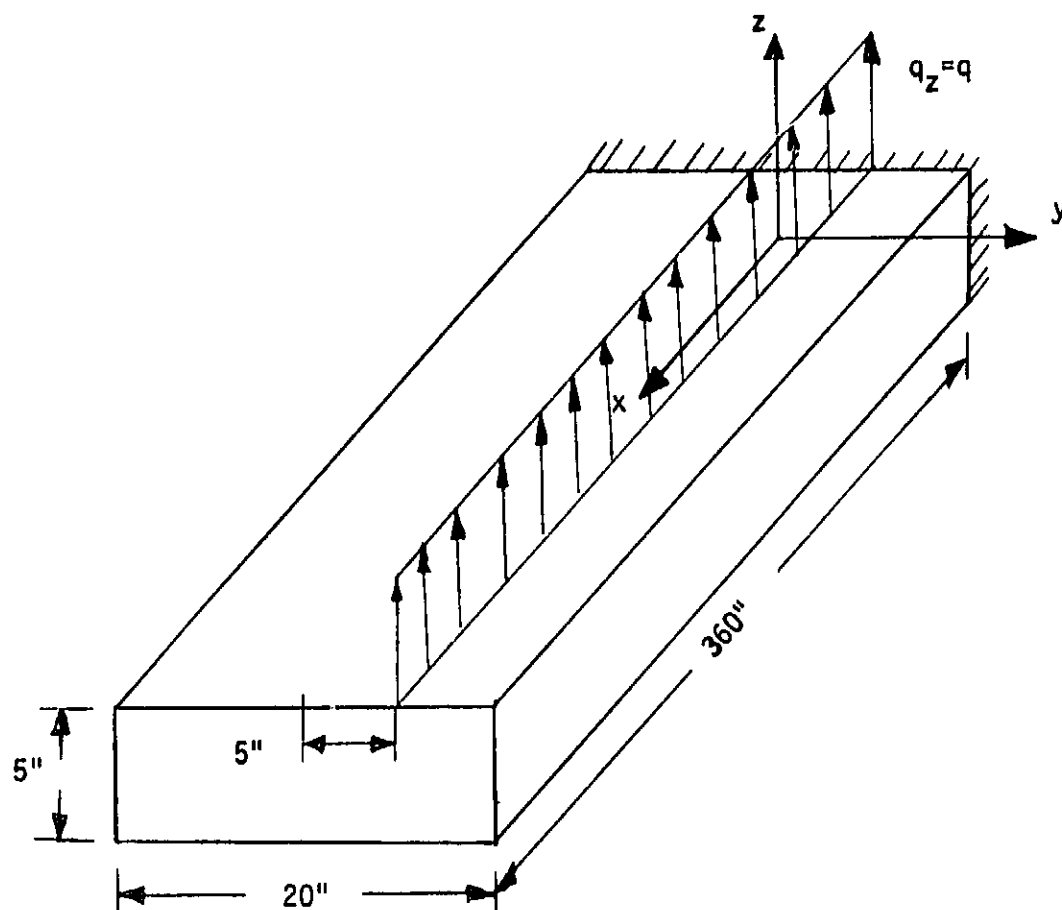
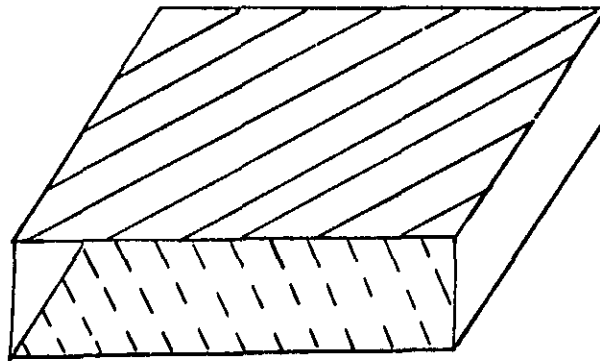
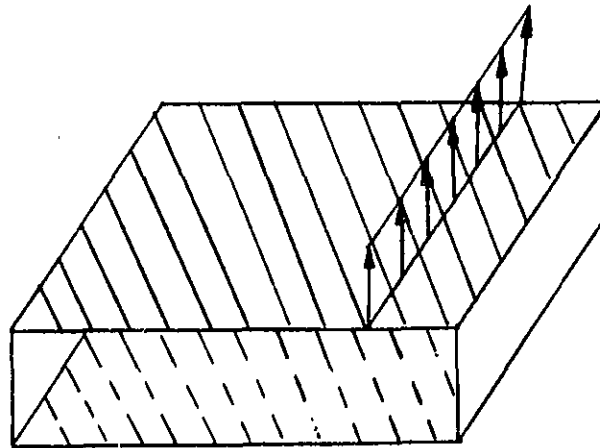


FIGURE 5. CH-47 ROTOR BLADE IDEALIZED AS A SINGLE CELL BEAM

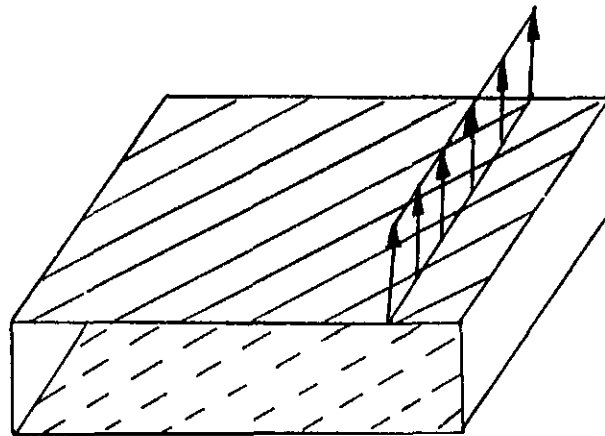
FIGURE 6. SKIN LAYUPS



BALANCED DESIGN



UNBALANCED DESIGN---POSITIVE COUPLING



UNBALANCED DESIGN----NEGATIVE COUPLING

Table I. Transverse Displacement at the Free End

Material	Skin Layout	Box Design	W/q			
			Classical (1)	Coupling (2)	Nonclassical (3)	Present (1)+(2)+(3)
GRAPHITE/ EPOXY	(0 <sub>12</sub> , 4 <sub>5</sub> 1 <sub>2</sub> )	Balanced	2.6876	0	0.0554	2.7430
		Positive Coupling	2.6876	0.0316	0.0554	2.7746
		Negative Coupling	2.6876	-0.0316	0.0554	2.7114
	(0 <sub>16</sub> , 4 <sub>5</sub> 8)	Balanced	2.2070	0	0.0593	2.2663
		Positive Coupling	2.2070	0.0220	0.0593	2.2883
		Negative Coupling	2.2070	-0.0220	0.0593	2.2443
GLASS/ EPOXY	(0 <sub>12</sub> , 4 <sub>5</sub> 1 <sub>2</sub> )	Balanced	7.7510	0	0.0507	7.8981
		Positive Coupling	7.7510	0.0464	0.0507	7.7553
		Negative Coupling	7.7510	-0.0464	0.0507	7.7971
	(0 <sub>16</sub> , 4 <sub>5</sub> 8)	Balanced	6.6383	0	0.0559	6.6942
		Positive Coupling	6.6383	0.0312	0.0559	6.7252
		Negative Coupling	6.6383	-0.0312	0.0559	6.6630

Table 2. Twist at the Free End

Material	Skin Layout	Box Design	$\phi/q$			
			Classical (1)	Coupling (2)	Nonclassical (3)	Present (1)+(2)+(3)
GRAPHITE/ EPOXY	$(0_{12}, 45_{12})$	Balanced	0.0017	0	0	0.0017
		Positive Coupling	0.0017	0.0032	-0.000033	0.0049
		Negative Coupling	0.0017	-0.0032	0.000033	-0.0015
	$(0_{16}, 45_8)$	Balanced	0.0018	0	0	0.0018
		Positive Coupling	0.0018	0.0022	-0.000032	0.0040
		Negative Coupling	0.0018	-0.0022	0.000032	-0.0037
GLASS/ EPOXY	$(0_{12}, 45_{12})$	Balanced	0.0015	0	0	0.0015
		Positive Coupling	0.0015	0.0046	-0.000016	0.0061
		Negative Coupling	0.0015	-0.0046	+0.000016	-0.0031
	$(0_{16}, 45_8)$	Balanced	0.0017	0	0	0.0017
		Positive Coupling	0.0017	0.0031	-0.000014	0.0048
		Negative Coupling	0.0017	-0.0031	0.000014	-0.0014

Table 3. Maximum Stress Resultants at the Root

Material	Skin Layup	Box Design	$N_x/q$			$N_{xy}/q$		
			Ref. (2)	Present	Ref. (2)	Present	Ref. (2)	Present
GRAPHITE/ EPOXY	$(0_{12}, 45_{12})$	Balanced	603	614	-593	-646	46.06	47.42
		Positive Coupling	598	622	-598	-621	46.37	46.15
		Negative Coupling	598	619	-598	-619	46.39	46.64
	$(0_{16}, 45_8)$	Balanced	603	611	-596	-625	46.09	47.32
		Positive Coupling	598	618	-598	-611	46.37	46.15
		Negative Coupling	598	615	-598	-610	46.39	46.61
GLASS/ EPOXY	$(0_{12}, 45_{12})$	Balanced	601	608	-594	-641	46.21	46.95
		Positive Coupling	598	611	-598	-618	46.38	46.24
		Negative Coupling	598	610	-598	-615	46.39	46.52
	$(0_{16}, 45_8)$	Balanced	600	605	-596	-619	46.24	46.82
		Positive Coupling	598	608	-598	-608	46.38	46.27
		Negative Coupling	598	607	-598	-607	46.39	46.49